A Molecular Dynamics Study of Tryptophan in Water

Pekka Mark and Lennart Nilsson*

Karolinska Institutet, Department of Bioscience, S-14157 Huddinge, Sweden

Received: April 18, 2002

Molecular dynamics simulations of a single tryptophan amino acid in water were performed with the CHARMM molecular mechanics program using the modified TIP3P, the refined SPC, and the original SPC/E water models. All these empirical water models are similar in nature, but small differences give significant differences in their properties for liquid water. Nanosecond molecular dynamics simulations were carried out in the NVT, NVE, or NPT ensembles using a cubic simulation cell furnished with periodic boundary conditions. The calculations of long-range interactions were performed with two different methods, the atom-based spherical cutoff method with force shifting, where the nonbonded interactions were smoothly shifted to zero at the cutoff distance, and the particle-mesh Ewald technique. Transition dipole autocorrelation functions and reorientation times of tryptophan were calculated and compared to experimental values. Tryptophan hydration was affected by the water model and the treatment of long-range electrostatic interactions. The reorientation time of tryptophan depended strongly on the water model used, and the viscosity of the model liquid was found to correlate with the tryptophan translational and rotational dynamics in water. Statistical accuracy and errors in the analyses are discussed.

1. Introduction

Tryptophan is the main fluorophore in natural proteins, and this has made the tryptophan residue one of most studied amino acids both experimentally[1−4] and theoretically.[1,5−8] The conformational space of a single tryptophan in water was studied by different NMR techniques,[3] and six low-energy conformations were obtained. One major conformation, the g^- conformation with the ring in an orientation perpendicular to the $C^\alpha-C^\beta$ bond,[9] was calculated to contain about 70% of all conformations.[3] The experimental rotational reorientation times for the single tryptophan residue and several tryptophan dipeptides and tripeptides in water at different temperatures and pH values have been obtained from fluorescence measurements of the tryptophan residue.[1] These experimental results were also compared to molecular dynamics simulations.[1] Several other molecular dynamics simulations of the tryptophan residue in water have previously been reported,[5−8] and the tryptophan residue is also a generally used fluorescence probe to monitor conformational dynamics of oligopeptide and protein conformations.[10−12]

This experimental knowledge of both the conformational space and the rotational reorientation time for the zwitterionic L-tryptophan in water makes it an attractive test system for comparison of different molecular dynamics simulation methods or models. In our previous study of the Ala-Pro dipeptide in water[13] we found that the rotational reorientation and the translational diffusion of the dipeptide was dependent on the water model used. Hydrogen bonding patterns between dipeptide and water were influenced by the water model, but the conformation of the dipeptide gave also significant effects.

In this study the zwitterionic L-tryptophan in its most populated conformation in water was used as a test molecule. Because the tryptophan interconverts between different conformations at a rate of a few events per nanosecond,[8] the comparison between different properties calculated from finite MD trajectories is more straightforward when the solute molecule is restricted to one conformation. Molecular dynamics simulations of the single tryptophan molecule in water using different water models, the modified TIP3P (transferable intermolecular potential 3P),[14,15] the refined SPC (simple point charge),[16] and the original SPC/E (extended simple point charge)[17] were performed using the CHARMM[18] molecular mechanics program. The water models used in this study are similar in nature and can be described as effective rigid pair potentials composed of Lennard-Jones (LJ) and Coulombic terms. Their slightly different geometries and LJ and Coulombic terms (Table 1) lead to significant differences in structural and dynamic properties for liquid water[19−22] (Table 2).

Molecular dynamics simulations in the NVT, NVE, or NPT ensembles, using a cubic simulation cell furnished with periodic boundary conditions were carried out. Two different methods for the calculation of long-range interactions were used, an atom-based spherical cutoff method with force shifting,[23] where the nonbonded interactions energies and forces were smoothly shifted to zero at the cutoff distance, and the particle-mesh Ewald technique.[24−26] We investigated the effects of the water model, the method to calculate long-range interactions, and the simulation ensemble on the hydration, rotational reorientation times, and translational diffusion of the zwitterionic L-tryptophan in water. To accomplish a meaningful comparison, with small estimated errors, a set of long simulations under identical conditions were performed and analyzed. In this study all trajectories were several nanoseconds long for high statistical accuracy; the equilibration time was longer than the whole trajectories in previously reported studies in the literature.[1,5−8]

2. Simulation Procedures

All molecular dynamics simulations and analyses were performed using the CHARMM[18] program and parameter set version 22.[27] Molecular dynamics simulations were carried out in the NVE (microcanonical), NVT (canonical), or NPT (isothermal−isobaric) ensembles, using a cubic simulation cell furnished with periodic boundary conditions. In the NPT

10.1021/jp025965e CCC: $22.00 © 2002 American Chemical Society
Published on Web 08/16/2002

TABLE 1: Nonbonded Parameters, Geometry and Electrostatic Properties of the Three-Point Water Models.

parameter	unit	TIP3P modified	SPC refined	SPC/E original
dipole	(Debye)	2.347	2.237	2.351
r_0OO	(Å)	3.5364	3.5257	3.5533
ϵ^{OO}	(kcal mol^{-1})	0.1521	0.1553	0.1553
r_0HH	(Å)	0.449	0	
ϵ^{HH}	(kcal mol^{-1})	0.046	0	
q^O	(e units)	−0.834	−0.8068	−0.8476
q^H	(e units)	0.417	0.4034	0.4238
b_0OH	(Å)	0.9572	1.0	1.0
θ_0HOH	(deg)	104.52	109.47	109.47

TABLE 2: Bulk Properties for Water Models at 25 °C

water model	TIP3P modified	SPC refined	SPC/E original	exp.
self-diffusion coefficient D[a] (10^{-9} m^2 s^{-1})	5.5	4.1	2.5	2.3[b]
tetrahedral structure[a]	increasing →			
viscosity (cP)	0.35[c]	0.54[d]	0.82[d]	0.83[d]
dielectric constant ϵ_0[e]	96.7	64.5	68.2	78.3
Kirkwood *G*-factor G_k[e]	5.25	3.71	3.70	
Debye relaxation time τ_D[e] (ps)	6.9	7.6	12.1	9.3
dipole (Debye)	2.347	2.237	2.351	

[a] Present calculation. [b] Reference 19. [c] Reference 20. [d] Reference 21. [e] Reference 22.

simulation, the pressure was controlled by coupling to an external pressure bath[28] at 1 atm using the isothermal compressibility[29] 0.0000455 atm^{-1}, with a coupling constant of 0.5 ps, and the temperature was coupled to a temperature bath[28] by a temperature coupling constant of 0.1 ps. In the NVE simulations, the temperature was allowed to vary ±5 K. In the NVT simulations, where the temperature was controlled with velocity rescaling, the temperature was also allowed to vary ±5 K. In the NVT simulations where the temperature was controlled with the Hoover extended system constant temperature algorithm[30−32] using a thermal piston with a "mass" of 100 kcal mol^{-1} ps^2. In all simulations, the SHAKE algorithm[33] was used to keep water molecules rigid. Integration of Newton's equations of motion was carried out with the Verlet leapfrog algorithm[24] with a time step of 0.002 ps. The dielectric constant was 1.0, and all coordinates were saved every 100 steps.

A total of 10 different MD simulations of a single tryptophan molecule in water were performed at 298 K (target temperature) using a solvent density 0.998 g/cm^3 in a cubic box with periodic boundary conditions (see Table 3). The single tryptophan molecule was placed in the middle of the box, with an edge of 30.0 Å, containing 901 H_2O molecules. All water molecules with the oxygen atom closer than 2.8 Å to any heavy atoms on tryptophan were removed. The tryptophan molecule was restricted to the most populated[3] conformation in water by using a harmonic restraint with a force constant 10.0 kcal mol^{-1} rad^{-1} on the dihedral angles $\chi_1 = -70°$, $\chi_2 = -75°$.

Three similar NVT ensemble simulations using different water models, the TIP3P[14,15] (modified), SPC[16] (refined), and SPC/E[17] (original), and one NPT ensemble simulation using the TIP3P[14,15] (modified) water model were carried out. To keep all bonds rigid in the tryptophan molecule the SHAKE algorithm was used. For the calculation of long-range interactions, an atom-based method with force shifting,[23] with a spherical cutoff of 12.0 Å, was used. The spherical nonbonded list was generated using a cutoff of 13.0 Å and was updated every 20 steps. The next three NVE simulations with different water models were performed using the SHAKE algorithm only on all covalent bonds of tryptophan molecule involving hydrogen atoms. The calculation of long-range interactions was performed with the atom-based method, force shifting with the spherical cutoff of 12.0 Å, but the spherical nonbonded list was generated for a 14.0 Å list and was updated every 10 steps. Each of these seven MD simulations was 4.0 ns long and was started with the same initial coordinates for all molecules.

Three other similar NVT simulations with different water models were performed using the SHAKE algorithm only on all covalent bonds of tryptophan molecule involving hydrogen atoms. The Ewald summation technique with the particle-mesh method[24−26] was used to calculate long-range interactions. The CHARMM implementation of the particle-mesh method was employed for simulated systems using $r_c = 12.0$ Å, $\kappa = 0.34$ Å^{-1}, and a grid spacing of 1 Å. The spherical nonbonded list was generated with a 14.0 Å cutoff and was updated when any atom had moved 1 Å or more. The temperature was controlled using the Hoover extended system constant temperature algorithm.[30−32] Each of these three simulations was 5.0 ns long and started with the same initial coordinates for all molecules. In all simulations in this study, the first 1.0 ns was used for equilibration and was not included in the analysis.

Hydration of the tryptophan molecule was estimated using the average number of hydrogen bonds to water, and their average lifetime, as the criteria for the hydration shell. The criteria used to define a hydrogen bond were hydrogen-to-acceptor distance ≤2.4 Å and acceptor-hydrogen-donor angle ≥135°. A water bridge was obtained when one water molecule had two hydrogen bonds with the tryptophan molecule at the same time. All hydrogen bonds were calculated from the trajectory with 5.0 ps time resolution.

The absorption and emission spectra of tryptophan are due to two low-lying exited states (^1L_a and ^1L_b), and the orientations of the ^1L_a and ^1L_b transition dipole moments are defined in the plane of the indole ring of tryptophan[5] as the vectors V1 and V2, respectively (Figure 1).

Rotational reorientation times for the tryptophan in water were calculated from anisotropy decay using the time-correlation function[34]

$$C(t_m) = \langle P_2[\mu_A(0)\cdot\mu_E(t_m)]\rangle$$

$$C(t_m) \approx \frac{1}{N-m}\sum_{n=1}^{N-m} P_2[\mu_A(t_n)\cdot\mu_E(t_n + t_m)]$$

where N is the total number of time steps in the simulations and m is the number of time steps passed at time t_m. P_2[- - - - -] is the second-order Legendre polynomial, and μ_A and μ_E are the absorption and emission unit transition dipole moment vectors, defined in the tryptophan molecule. The exited state ^1L_a was assumed to have the absorption and emission unit transition dipole moment vectors at the same position. For the exited state ^1L_b, the same approximation was used. Here the rotational reorientation times were calculated using both V1 and V2 (Figure 1). We calculated the rotational reorientation time τ from the inverse of the slope of the linear part, 1 ps < t_m < 10 ps, of the decay of ln[$C(t_m)$] with time t_m.

The translational diffusion coefficient for the tryptophan in water was calculated from the mean square displacement (MSD) of the C_γ atom, which is near the center of mass of tryptophan. The Einstein relation,[34]

$$\lim_{t\to\infty}\langle|\mathbf{r}(t' + t) - \mathbf{r}(t')|^2\rangle = 6Dt$$

was used, where $\mathbf{r}(t)$ is the position of the C_γ atom in the

TABLE 3: Systems Simulated

simulation	water model	ensemble	temperature control	nonbonded interactions	simulation period [ns]
1	TIP3P modified	NVT	velocity scaling	force shift 12.0 Å	4.0[a]/3.0[b]
2	SPC refined	NVT	velocity scaling	force shift 12.0 Å	4.0/3.0
3	SPC/E original	NVT	velocity scaling	force shift 12.0 Å	4.0/3.0
4	TIP3P modified	NPT	Berendsen thermostat	force shift 12.0 Å	4.0/3.0
5	TIP3P modified	NVE	no temp. control	force shift 12.0 Å	4.0/3.0
6	SPC refined	NVE	no temp. control	force shift 12.0 Å	4.0/3.0
7	SPC/E original	NVE	no temp. control	force shift 12.0 Å	4.0/3.0
8	TIP3P modified	NVT	Hoover thermostat	Ewald 12.0 Å	5.0/4.0
9	SPC refined	NVT	Hoover thermostat	Ewald 12.0 Å	5.0/4.0
10	SPC/E original	NVT	Hoover thermostat	Ewald 12.0 Å	5.0/4.0

[a] Total time. [b] Time used for analysis.

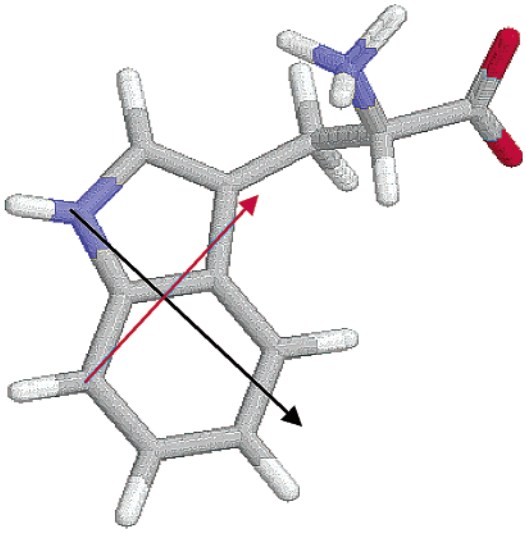

Figure 1. Zwitterionic L-tryptophan in water; the major conformation, the g^- conformation with the ring in an orientation perpendicular to the $C^{\alpha}-C^{\beta}$ bond. The orientations of the ^1L_a and ^1L_b transition dipole moments are defined in the plane of the indole ring of tryptophan as the vectors V1 (black) and V2 (red), respectively.

tryptophan molecule at time t, D is the translational diffusion coefficient, and the brackets denote the averaging over the time origins t'.

The self-diffusion coefficient for water was calculated using the MSD of the oxygen atom of all the water molecules.

3. Results

3.1. Temperature, Stability, and Equilibration. In simulations #1, #2, and #3, where the nonbonded interactions were treated using the force shift with the spherical cutoff radius of 12.0 Å together with the spherical nonbonded list with the cutoff radius of 13.0 Å and updated every 20 steps, the velocity scaling was used to keep the system temperature at the target temperature of 298 K. In all three simulations the system temperature was slightly over the target temperature (Table 4). In simulation #4, where the Berendsen thermostat algorithm together with the pressure control was used, the trajectory has exactly the target temperature of 298 K. In simulations #5, #6, and #7, where the nonbonded interactions were treated using the force shift with the spherical cutoff radius of 12.0 Å but the spherical nonbonded list with the radius of 14.0 Å and updated every 10 steps was used, the velocity scaling was not needed to stabilize the system temperature to the target temperature of 298 K. In simulations #8, #9, and #10, where the nonbonded interactions were treated using the Ewald summation technique with the particle-mesh method and the temperature was controlled with the Hoover thermostat, the trajectories have exactly the target temperature of 298 K.

The radial distribution functions, g_{OO}, g_{OH}, and g_{HH} (not shown here), and the calculated self-diffusion coefficients of water from simulations #5, #6, and #7 (see Table 4) were similar when compared with pure water simulations.[35] Slightly lower self-diffusion coefficients were found with simulations #8, #9, and #10 with the particle-mesh Ewald technique when compared with other simulations in this study. In these simulations the system pressure was slightly lower for TIP3 than for SPC or SPC/E (Table 4).

3.2. Tryptophan Hydration. Hydration of the tryptophan was calculated from all trajectories, using the last 3.0 ns of each one for investigation. All calculated hydrogen bonds to water and water bridges from the simulations are given in Table 5. Hydration of the tryptophan was found to depend on the water model. The tryptophan was most hydrated with the TIP3P water model when the simulations with the rigid tryptophan were compared. The number of water molecules making the hydrogen bonds with the rigid tryptophan molecule were significantly higher when the calculations with the TIP3P water model were compared with the other water models. The number of water molecules making the hydrogen bonds with the rigid tryptophan molecule was decreased when the Berendsen thermostat was used.

The more flexible tryptophan model was most hydrated with the SPC/E water model when NVE simulations were compared, but the tryptophan was the least hydrated with the SPC/E water model when NVT simulations with Hoover thermostat and Ewald summation were compared. The longest lifetime of the hydrogen bonds was obtained with the SPC/E water model. In our previous study with the dipeptide Ala-Pro in water,[13] the SPC/E water model has also the longest lifetime of the hydrogen bonds. The number of the water bridges was low for all simulations in this study.

3.3. Rotational and Translational Diffusion. Mean values and standard deviations for the rotational reorientation times of the unit vectors V1 and V2 were calculated from three (simulations #1 to #7) or four (simulations #8 to #10) nonoverlapping blocks of 1.0 ns. $C(t_m)$ was found to decay exponentially with time, and the rotational reorientation time τ (Table 6) was calculated from the inverse of the slope of the linear decay of $\ln[C(t_m)]$ with time t_m (Figure 2). The rotational reorientation times for 1.0 ns blocks from simulations #8, #9, and #10 have standard deviations of 13%, 5%, and 5% for V1 and for V2 4%, 4%, and 9%, respectively, when the TIP3P, SPC, and SPC/E water models were used. The error in the estimates from the total trajectory will be roughly half as large.

We found that the rotational reorientation of the vector V1 was always faster than the vector V2, consistent with previously reported results in the literature.[1,5,8] The experimental value[1]

TABLE 4: Simulation Results

simulation	temp control	temp[a] (K)	total pot. E[a] (kcal/mol)	system pressure[a] (bar)	D[b] (10^{-9} m^2 s^{-1})
1	yes 273/3000 ps[c]	301.3 (1.74)	−8476.5 (14.3)		5.9
2	yes 197/3000 ps	301.0 (1.79)	−8565.3 (16.7)		4.4
3	yes 126/3000 ps	300.5 (1.83)	−9644.6 (18.3)		2.8
4	Berendsen thermostat	298.0 (0.27)	−8528.2 (15.0)	1.0 (6.9)	5.6
5	no	298.4 (0.99)	−8502.9 (5.3)		5.6
6	no	299.0 (1.13)	−8583.3 (6.1)		4.3
7	no	297.7 (1.39)	−9688.9 (8.3)		2.6
8	Hoover thermostat	298.0 (0.03)	−8743.2 (15.0)	−247.8 (99.5)	5.5
9	Hoover thermostat	298.0 (0.03)	−8832.8 (18.6)	21.1 (109.4)	4.1
10	Hoover thermostat	298.0 (0.03)	−9948.5 (23.0)	27.1 (132.5)	2.5

[a] Average calculated over the analyzed part of the trajectory; standard deviation in parentheses. [b] Mean value of self-diffusion coefficient for water with standard deviation = 0.1×10^{-9} m^2 s^{-1}. [c] Number of velocity rescaling events over the analyzed part of the trajectory.

TABLE 5: Hydrogen Bonds to Water and Water Bridges

simulation	HT1	HT2	HT3	HE1	OT1	OT2	OT−OT	OT1−HT
1	0.83[a]/9.7[b]	0.84/9.0	0.86/10.4	0.60/5.6	2.33/7.2	2.69/8.1	0.27/5.6	0.04/5.0
2	0.73/10.1	0.67/9.4	0.74/9.4	0.46/5.9	1.98/8.4	2.37/9.2	0.21/5.9	0.07/5.0
3	0.78/12.3	0.73/10.8	0.75/12.9	0.46/6.1	2.05/10.3	2.41/12.1	0.18/5.6	0.05/5.2
4	0.71/10.1	0.74/9.4	0.72/9.6	0.49/5.6	2.06/7.0	2.43/8.0	0.18/5.4	0.05/5.0
5	0.63/9.2	0.65/8.7	0.62/8.9	0.46/5.8	1.53/7.1	1.76/7.6	0.17/5.5	0.04/5.0
6	0.72/9.6	0.71/9.7	0.69/9.2	0.53/5.8	1.85/8.4	2.17/9.2	0.16/5.3	0.05/5.0
7	0.79/12.1	0.79/13.0	0.81/13.4	0.53/6.4	2.26/10.5	2.69/12.9	0.21/5.5	0.06/5.1
8	0.70/10.3	0.62/9.4	0.69/9.5	0.50/5.6	1.91/7.2	2.17/7.7	0.17/5.8	0.06/5.2
9	0.74/9.0	0.70/9.3	0.70/9.3	0.43/5.9	1.72/8.4	2.03/9.8	0.13/5.4	0.06/5.1
10	0.61/11.6	0.57/12.2	0.57/10.9	0.40/6.6	1.45/10.5	1.94/12.6	0.13/5.4	0.04/5.2

[a] Average number. [b] Average lifetime (ps).

TABLE 6: Rotational Reorientation and Translational Diffusion of Tryptophan

simulation	rotational reorientation time (ps) V1	rotational reorientation time (ps) V2	translational diffusion (10^{-9} m^2 s^{-1})
1	15.2(2.0)[a]	21.7(2.2)[a]	
	15.1[b]	21.7[b]	1.0[c]
2	19.4 (0.8)	27.3 (1.2)	
	19.4	27.4	1.0
3	28.4 (6.9)	43.4 (3.1)	
	27.5	43.3	0.5
4	16.5 (1.9)	22.4 (2.1)	
	16.3	22.3	1.1
5	17.8 (2.3)	22.3 (2.2)	
	17.6	22.3	1.1
6	20.9 (2.4)	28.6 (1.3)	
	20.7	28.5	0.9
7	28.8 (2.0)	42.8 (2.7)	
	28.6	42.6	0.5
8	16.6 (2.2)	22.9 (1.0)	
	16.4	22.9	1.3
9	23.3 (1.2)	31.6 (1.5)	
	23.3	31.5	0.8
10	34.0 (1.7)	45.4 (4.1)	
	33.9	45.2	0.4

[a] The mean value and standard deviation (in parentheses) of the rotational reorientation of the V1 and V2 vectors were calculated using nonoverlapping blocks of 1.0 ns. [b] The rotational reorientation of the V1 and V2 vectors were calculated from the whole 3.0 ns trajectories. [c] The translational diffusions for tryptophan were calculated from the whole 3.0 ns trajectories.

for the rotational reorientation time of tryptophan at 298 K is 21.8 ± 1.2 ps, but this value is strongly temperature dependent (Table 7). When comparing our simulation results with the experimental rotational reorientation times of tryptophan in water (Figure 3), the SPC (refined) water model has the best

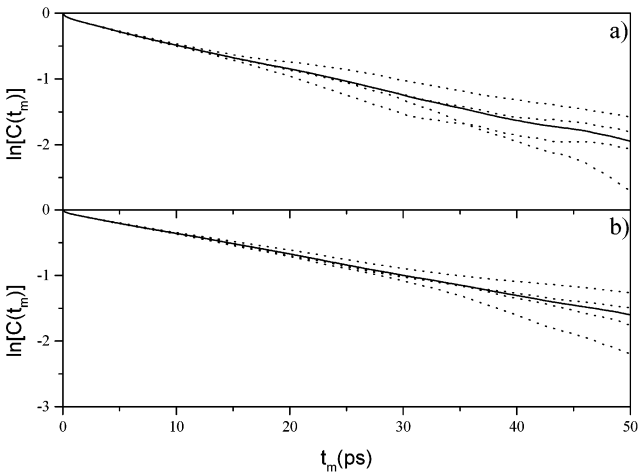

Figure 2. Time correlation function $C(t_m)$ as a function of time (t_m) from simulation #9 with SPC (refined) water model. (a) ln[$C(t_m)$] calculated with vector V1, (b) ln[$C(t_m)$] calculated with vector V2. ln-[$C(t_m)$] was calculated from nonoverlapping blocks of 1.0 ns (dot) or from the full 4.0 ns simulation (line).

rotational reorientation times. The TIP3P (modified) water model simulations gave too high rotational reorientation times and the SPC/E water model simulations gave too low rotational reorientation times. The calculated rotational reorientation times for tryptophan were of the same magnitude as the rotational reorientation times of the Ala-Pro dipeptide in water[13] as expected, since the single tryptophan molecule has approximately the same radius of gyration as the Ala-Pro dipeptide: 3.14, 2.80, and 2.75 Å for the tryptophan, the Ala-Pro trans isomer, and the Ala-Pro cis isomer, respectively. The rotational reorientation time of the tryptophan increases with increasing viscosity of the model liquids.

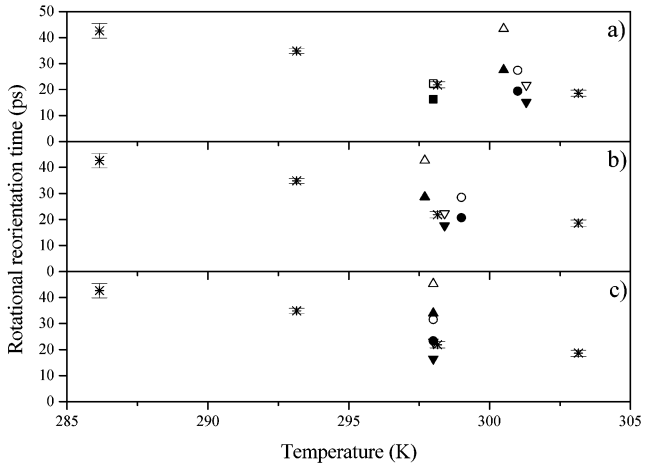

Figure 3. Rotational reorientation time of zwitterionic L-tryptophan in water calculated with vector V1 (solid) and vector V2 (open). (a) simulation #1 down triangle, simulation #2 circle, simulation #3 up triangle, and simulation 4# square. (b) simulation #5 down triangle, simulation #6 circle, and simulation #7 up triangle. (c) simulation #8 down triangle, simulation #9 circle, and simulation #10 up triangle. Experimental values: star with error bars.

TABLE 7: Experimental Rotational Reorientation Times for Tryptophan at Different Temperatures

temp (K)	rotational reorientation time (ps)
303	18.6 ± 1.2
298	21.8 ± 1.2
293	34.8 ± 1.0
286	42.6 ± 2.8

The translational diffusion coefficient of the tryptophan molecule was estimated from the long time slope of the mean square displacement. The accuracy decreases for longer times, due to the decrease in the sampling, and at very short times the Einstein relation is not valid. For this reason the intermediate interval, 4−100 ps, where the plot of MSD vs time is linear, was used to calculate the translational diffusion coefficients (Table 6). The translational diffusion coefficient of the tryptophan was also found to depend on the viscosity of the water models (Table 2).

4. Summary and Discussion

All results in this study gave the same conclusion: the viscosity of the water model is the property that rules the diffusion properties of the tryptophan in water. Similar results were also found in our previous study with the dipeptide Ala-Pro in water.[13] The water model with the highest viscosity has a low self-diffusion coefficient and a good structure of the model liquid compared to experiments. It should be noted here that the SPC/E water model has the best bulk water properties of the water models tested in this study, when compared with the experimental values.

In our tryptophan simulations the SPC (refined) water model together with the all-atom CHARMM 22 force field[27] for the tryptophan molecule gave the best rotational reorientation time when compared with the other water models. The TIP3P (modified) water model simulations gave too high rotational reorientation times and the SPC/E water model simulations gave too low rotational reorientation times compared with the experimental values. The rotational reorientation time was also influenced by the choice of transition dipole moment vector, the treatment of the nonbonded interactions, and the simulation ensemble. These effects were, however, not of the same magnitude as the effect of the viscosity. Daura et al.[8] compared SPC with SPC/E, and they found that the GROMOS96 force field[36] with a reaction field correction for long-range electrostatic interactions gave the best agreement with experimental reorientation times for SPC/E, with SPC giving about twice as fast rotation. Since the water models are the same, with very similar properties under the simulation conditions used by us and by Daura et al.,[8] the reason for this difference is probably differences in the force field description of tryptophan.

Hydration of the tryptophan was also found to depend on the water model, the treatment of nonbonded interactions, and the simulation ensemble, but not directly on the viscosity. The hydration of tryptophan depends on the balance between the water−water and water−tryptophan interactions, which is a complicated process where the water model properties, such as the partial charges, nonbonded parameters, and the geometry of the water models are connected with the treatment of nonbonded interactions and the simulation ensemble effects. More investigations are needed to get a clear picture of this complicated problem.

Acknowledgment. We thank Dr. Jan Norberg for critical reading of the manuscipt. This work was supported by the Magnus Bergvall Foundation, the Swedish Natural Science Research Council, and the Swedish Research Council for Engineering Science.

References and Notes

(1) Chen, L. X.-Q.; Engh, R. A.; Fleming, G. R. *J. Phys. Chem.* **1988**, *92*, 4811−4816.
(2) Shen, X.; Knutson, J. R. *J. Phys. Chem. B* **2001**, *105*, 6260−6265.
(3) Dezube, B.; Dobson, C. M.; Teague, C. E. *J. Chem. Soc., Perkin Trans. 2* **1981**, 730−735.
(4) Cao, X.; Fischer, G. *J. Phys. Chem. A* **1999**, *103*, 9995−10003.
(5) Hu, Y.; Fleming, G. R. *J. Phys. Chem.* **1991**, *94*, 3857−3866.
(6) Gordon, H. L.; Jarrell, H. C.; Szabo, A. G.; Willis, K. J.; Somorjai, R. L. *J. Phys. Chem.* **1992**, *96*, 1915−1921.
(7) Simonson, T.; Wong, C. F.; Brünger, A. T. *J. Phys. Chem. A* **1997**, *101*, 1935−1945.
(8) Daura, X.; Suter, R.; van Gunsteren, W. F. *J. Chem. Phys.* **1999**, *110*, 3049−3055.
(9) Markley, J. L.; Bax, A.; Arata, Y.; Hilbers, C. W.; Kaptein, R.; Sykes, B. D.; Wright, P. E.; Wüthrich, K. *J. Biomol. NMR* **1998**, 12, 1−23.
(10) Elofsson, A.; Rigler, R.; Nilsson, L.; Roslund, J.; Krause, G.; Holmgren, A. *Biochemistry* **1991**, *30*, 9648−9656.
(11) Antonini, P. S.; Hillen, W.; Ettner, N.; Hinrichs, W.; Fantucci, P.; Doglia, S. M.; Bousquet, J.-A.; Chabbert, M. *Biophys. J.* **1997**, *72*, 1800−1811.
(12) Burkhard, P.; Hommel, U.; Sanner, M.; Walkinshaw, M. D. *J. Mol. Biol.* **1999**, *287*, 853−858.
(13) Mark, P.; Nilsson, L. *J. Phys. Chem. B* **2001**, *105*, 8028−8035.
(14) Jorgensen, W. L.; Chandrasekhar, J.; Madura, J. D.; Impey, R. W.; Klein, M. L. *J. Chem. Phys.* **1983**, *79*, 926−935.
(15) Neria, E.; Fischer, S.; Karplus, M. *J. Chem. Phys.* **1996**, *105*, 1902−1921.
(16) Berweger, C. D.; van Gunsteren, W. F.; Müller-Plathe, F. *Chem. Phys. Lett.* **1995**, *232*, 429−436.
(17) Berendsen, H. J. C.; Grigera, J. R.; Straatsma, T. P. *J. Phys. Chem.* **1987**, *91*, 6269−6271.
(18) Brooks, B. R.; Bruccoleri, R. E.; Olafson, B. D.; States, D. J.; Swaminathan, S.; Karplus, M. *J. Comput. Chem.* **1983**, *4*, 187−217.
(19) Mills, R. *J. Phys. Chem.* **1973**, *77*, 685−688.
(20) Feller, S. E.; Pastor, R. W.; Rojnuckarin, A.; Bogusz, S.; Brooks, B. R. *J. Phys. Chem.* **1996**, *100*, 17011−17020.
(21) Smith, P. E.; van Gunsteren, W. F. *Chem. Phys. Lett.* **1993**, *215*, 315−318.
(22) Höchtl, P.; Boresch, S.; Bitomsky, W.; Steinhauser, O. *J. Chem. Phys.* **1998**, *109*, 4927−4937.
(23) Steinbach, P. J.; Brooks, B. R. *J. Comput. Chem.* **1994**, *15*, 667−683.
(24) van Gunsteren, W. F.; Berendsen, H. J. C. *Angew. Chem., Int. Ed. Engl.* **1990**, *29*, 992−1023.

(25) Sagui, C.; Darden, T. A. *Annu. Rev. Biophys. Biomol. Struct.* **1999**, *28*, 155−179.

(26) Ewald, P. *Ann. Phys.* **1921**, *64*, 253.

(27) MacKerell, A. D., Jr.; Bashford, D.; Bellott, M.; Dunbrack Jr:, R. L.; Evanseck, J. D.; Field, M. J.; Fischer, S.; Gao, J.; Guo, H.; Ha, S.; Joseph-McCarthy, D.; Kuchnir, L.; Kuczera, K.; Lau, F. T. K.; Mattos, C.; Michnick, S.; Ngo, T.; Nguyen, D. T.; Prodhom, B.; Reiher, W. E., III.; Roux, B.; Schlenkrich, M.; Smith, J. C.; Stote, R.; Straub, J.; Watanabe, M.; Wiórkiewicz-Kuczera, J.; Yin, D.; Karplus, M. *J. Phys. Chem. B* **1998**, *102*, 3586−3616.

(28) Berendsen, H. J. C.; Postma, J. P. M.; van Gunsteren, W. F.; DiNola, A.; Haak, J. R. *J. Chem. Phys.* **1984**, *81*, 3684−3690.

(29) CRC Handbook of chemistry and physics, 73th ed.; Lide, D. R., Ed.; CRC Press: Boca Raton, 1992−1993.

(30) Hoover, W. G. *Phys. Rev.* **1985**, *A31*, 1695−1697.

(31) Nosé, S. *Mol. Phys.* **1984**, *52*, 255−268.

(32) Nosé, S. *J. Phys.: Condens. Matter* **1990**, *2*, 115−119.

(33) Ryckaert, J.-P.; Ciccotti, G.; Berendsen, H. J. C. *J. Comput. Phys.* **1977**, *23*, 327−341.

(34) Allen, M. P.; Tildesley, D. J. *Computer Simulations of Liquids*; Oxford Science: Oxford, 1987.

(35) Mark, P.; Nilsson, L. *J. Phys. Chem. A* **2001**, *105*, 9954−9960.

(36) van Gunsteren, W. F.; Billeter, S. R.; Eising, A. A.; Hünenberger, P. H.; Krüger, P.; Mark, A. E.; Scott, W. R. P.; Tironi, I. G. *Biomolecular Simulation: The GROMOS96 Manual and User Guide* **1996**, (vdf Hochschulverlag AG an der ETH Zürich and BIOMOS b. v., Zürich, Groningen, 1996).